

## Article

# Power Compensation Strategy and Experiment of Large Seedling Tree Planter Based on Energy Storage Flywheel

Binhai Zhu, Jiuqing Liu \*, Chunmei Yang, Wen Qu and Peng Ding

School of Mechanical and Electrical Engineering, Northeast Forestry University, Harbin 150040, China; zhubinhai1987@163.com (B.Z.); ycmnefu@126.com (C.Y.)

\* Correspondence: nefujdljq@163.com

**Abstract:** The intermittent hole-digging tree-planting machine shows a periodic short-time peak load law in planting operation, and the operation process is “idling” for small loads most of the time, leading to large torque fluctuations in the transmission system, unscientific power matching, and high energy consumption. To solve the above problems, this article proposes to use a series of energy-saving flywheels in the transmission system of the tree planting machine. On the premise of obtaining holes that meet the target young tree planting requirements, the optimal power compensation strategy for the flywheel system of the tree planting machine is studied to reduce torque fluctuations in the power transmission system, use smaller power drive units, and save energy. Firstly, the nonlinear multi-body dynamics simulation model of soil cutting by the hole-digging component is established. The boundary and contact conditions are set to simulate the power consumption of the hole-digging component at three rotating speeds. Based on the simulation results, the flywheel power compensation strategy is discussed, and the torque fluctuation of the flywheel balance system is analyzed. The results showed that the higher the speed, the greater the power consumption. The power value suddenly increased from 17.82 kW (1.28 s) to 27.93 kW (1.43 s) when the speed was 220 r/min. Then, the power value rapidly decreased, and the power consumption presented a short-term peak feature. The transmission system’s maximum input power is determined as 17.82 kW according to the various simulated power consumption characteristics. The part exceeding the power consumption is compensated by the energy storage flywheel. The total compensation energy was 2382.5 J. After the flywheel system was involved, the maximum output power of the tractor power output shaft decreased by 36.2%, and the peak torque decreased from 445.7 N·m to 285.1 N·m. The power consumption obtained from the field test and simulation was similar, but the energy required to overcome peak load was jointly provided by the flywheel and the engine. The actual input power of the power output shaft during the energy release period of the flywheel system was 18.51 kW when the rotating speed of the hole-digging component was 220 r/min, and the relative error with the simulation value was 2.43%. The measured actual speed reduction of the flywheel system was 8.9%. After installing an energy storage flywheel in the transmission system of the tree planting machine, the output power of the power unit can be stabilized. Tree planting machines can be equipped with smaller power units, which can reduce energy consumption and exhaust emissions.

**Keywords:** tree planting machine; multibody dynamics; flywheel; power; experiments



**Citation:** Zhu, B.; Liu, J.; Yang, C.; Qu, W.; Ding, P. Power Compensation Strategy and Experiment of Large Seedling Tree Planter Based on Energy Storage Flywheel. *Forests* **2023**, *14*, 1039. <https://doi.org/10.3390/f14051039>

Academic Editor: Gianni Picchi

Received: 13 March 2023

Revised: 3 May 2023

Accepted: 10 May 2023

Published: 18 May 2023



**Copyright:** © 2023 by the authors. Licensee MDPI, Basel, Switzerland. This article is an open access article distributed under the terms and conditions of the Creative Commons Attribution (CC BY) license (<https://creativecommons.org/licenses/by/4.0/>).

## 1. Introduction

Seedling transplanting is a method of efficiently transplanting seedlings from the nursery to the planting site. Transplanting can increase the spacing and row spacing between seedlings, expand their survival space, and cut off their main and larger lateral roots during the transplanting process. Consequently, a large number of horizontal roots and fibrous roots can be produced from the broken root section, thus improving the survival rate of seedlings [1,2].

China transplants many seedlings from fast-growing and high-yielding timber forests every year. With the “double carbon” goal, simple and extensive transplanting machinery is far from meeting the current demand. More innovative and advanced technologies need to be developed for seedling transplanting equipment. However, the development of equipment technology and energy conservation and efficiency improvement technology will be the trends in the development of agricultural and forestry equipment. The energy conservation and emission reduction methods mainly include efficient matching of equipment, preventive maintenance, and energy conservation using new technologies [3–5]. Intermittent digging and transplanting machines are important ecological transplants, mainly implemented by matching high-power tractors. This transplanting machine has an intermittent load, i.e., it only bears the working peak load for a short time during a period of digging and planting seedlings, and most of the time it is “idling” with a small load. If the tractor is selected according to the working load, the tractor’s power will be large. Rough statistics show that the selected power of the tractor is more than 3–5 times the average power in the work cycle. Because power matching is usually ignored during the design of machines and tools, serious energy waste is caused [6,7]. At the same time, the frequent rise and fall of the load greatly impacts the tractor transmission system and reduces the service life of the parts. Experienced tractor operators must adjust the throttle opening frequently according to the load fluctuation during operation, and the tractor often emits black smoke. Therefore, it is of great significance to conduct in-depth research on the collection and release of energy during afforestation equipment operations in order to improve energy utilization efficiency [8–10].

Energy storage technology is the main way to improve equipment stability, energy conservation, and consumption reduction. Typical energy storage technologies mainly include physical and chemical storage [11,12]. With the rise of energy storage technology, flywheel energy storage, with its advantages of fast response, unlimited power, small size, and ease of movement, has been gradually developed and applied in various fields. It has been used in the automotive field at an early stage and is also widely used in UPS, subway energy recovery, electric vehicles, electric peak shaving, and other fields [13]. In the application of mechanical flywheel hybrid power systems in automobiles, the energy transfer efficiency is better than that of electric drive systems because the energy conversion form between the flywheel and the transmission system has not changed. When the vehicle decelerates, the kinetic energy of the vehicle transmission system is directly stored in the flywheel in the form of mechanical energy. When accelerating or climbing, the rotating flywheel, as an auxiliary power source, is dynamically coupled with the transmission system through the clutch (or CVT) to provide instantaneous high-power compensation for the engine [14,15]. The drilling rig is the key piece of equipment for petroleum exploration, with an annual consumption of more than 1.5 million tons of diesel. After the intervention of an advanced energy storage system, it can significantly improve the drilling rig’s ability to cope with complex conditions, and the impact load damage to equipment can be greatly decreased. The generator’s fuel efficiency can also apparently be improved. Accordingly, energy conservation and emission reduction can be achieved by feeding the potential energy of tripping back into the flywheel and releasing it when lifting the drill [16].

In this paper, aiming at the transplanting of large seedlings such as 2–3-year-old fruit seedlings and poplar seedlings to solve the impact of periodic short-time peak load of the intermittent hole-digging tree-planting machine and save energy, an effective method of installing an energy flywheel in the transmission system of the tree-planting machine is proposed. The energy storage flywheel will store energy from the power output shaft at low loads and release energy at short peak loads, leading to an apparent decrease in the loading rate of the engine. Firstly, the flywheel energy storage system is designed for intermittent digging and transplanting machines. Then, the nonlinear multi-body dynamic simulation model of digging parts and cutting soil is established. Finally, the boundary and contact conditions are set to simulate the power consumption during the intermittent digging process. Based on the simulation results, the flywheel power compensation strategy is

discussed, the torque fluctuation after the flywheel intervention is analyzed, and the field verification test is carried out. This study provides a reference for optimizing the power matching between the tractor and the implement, reducing transmission torque fluctuation, and realizing energy savings and consumption reduction.

## 2. Materials and Methods

### 2.1. Description of the Tree Planting Machine

As shown in Figure 1, the tree planting machine mainly includes a transmission system, control system, soil covering device, compaction device, young tree support device, frame, etc. The transmission system mainly includes universal joint cross shaft assembly I, double output shaft gearbox, hydraulic pump, electromagnetic clutch I, bearing seat, flywheel fixed lock nut set, flywheel set, electromagnetic clutch II, universal joint cross shaft assembly II, single output shaft gearbox, burr parts, and the gearbox. Its purpose is to transfer the torque and speed of the tractor power output shaft to the digging parts and simultaneously drive the hydraulic pump to run.

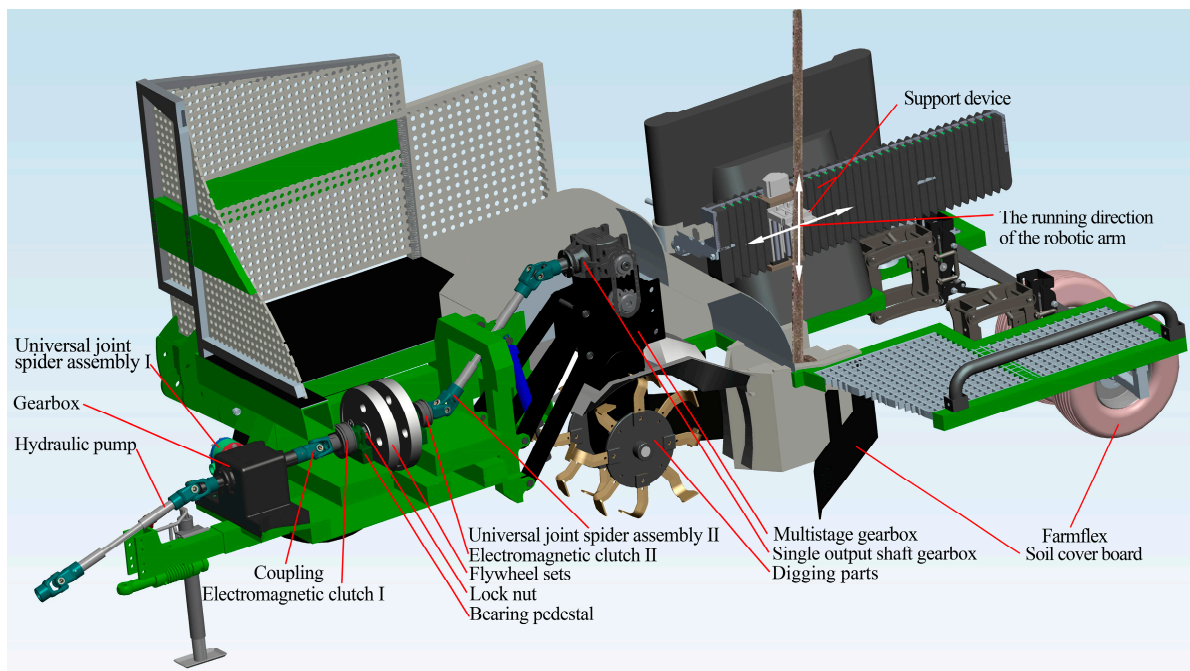


**Figure 1.** Three-dimensional modeling of a tree planting machine.

The intermittent hole-digging and transplanting mechanism is shown in Figure 2. Point (O) is the tractor traction point. During the young tree planting operation, the tractor pulls the transplanting machine to continuously run at a certain speed. The tractor drives the hole-digging parts to rotate and cut the soil through the transmission system. The machine's initial state is shown in the dotted line position of Figure 2. The floating cylinder (BE) is controlled to contract through the hydraulic system, and the hole-digging cylinder (CK) is extended. The frame and the hole-digging parts move down simultaneously, and the rotated blade cuts the soil. After the frame falls to the lowest position (at the solid line of the mechanism), it stops moving, and the hole-digging cylinder continues to extend. When the hole reaches the predetermined depth, the controller detects the sensor signal, The oil cylinder immediately runs in reverse, driving the excavation component to quickly lift above the ground. As shown in Figure 1, the robotic arm quickly throws the saplings into the hole, and the soil cover plate is used to backfill the soil into the hole. To prevent the root of the hole, the robotic arm drives the saplings to vibrate upwards and lift for a certain distance. During this process, the young tree support device runs backwards under the drive of a servo motor, and the mechanical arm always clamps the seedlings to ensure their

verticality. When the compaction wheel compacts the soil at the root of the seedlings, the mechanical arm releases the seedlings, and the seedling support device quickly returns to its initial position. Then, the floating oil cylinder (BE) extends to raise the frame, completing one planting cycle: hole forming. The parameters of the tree planting machine are shown in Table 1. The working process of the transmission system is as follows: Start the tractor and put the PTO operating handle in the combined position, where the hydraulic pump ensures that the digging parts are raised to the highest point. First, at the low speed of the PTO, enable the electromagnetic clutch I, causing the flywheel energy storage device to operate. Then, enable the electromagnetic clutch II to rotate the digging cutter. By adjusting the throttle opening of the tractor, the predetermined output power and speed can be reached.

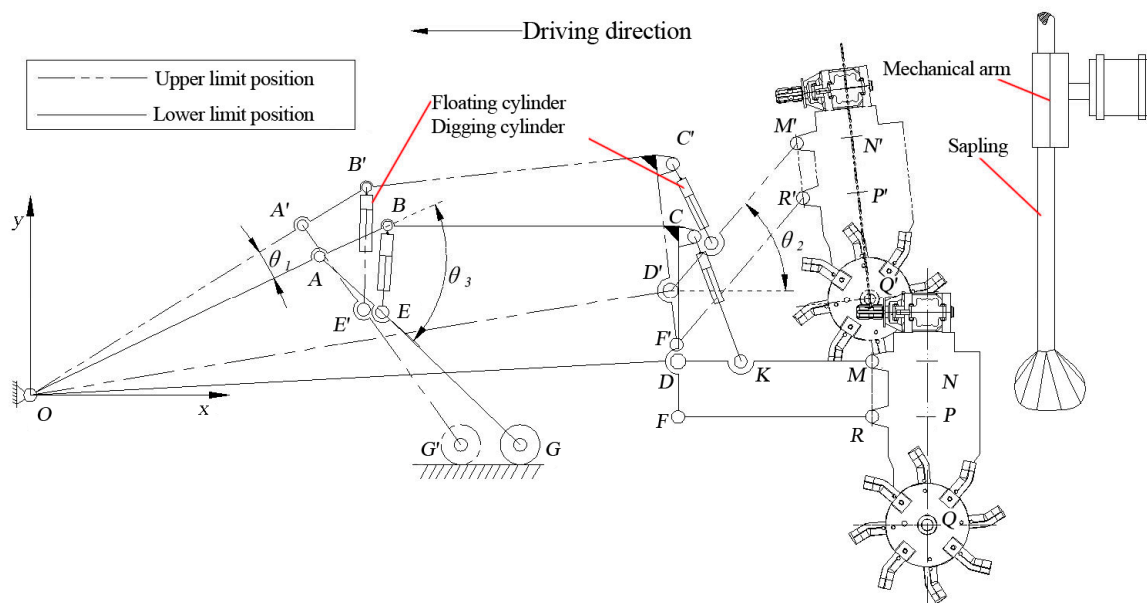


Figure 2. Schematic diagram of the intermittent digging mechanism.

Table 1. Hole-forming parameters of the tree planting machine.

Parameter	Value	Parameter	Value
Diameter of cutterhead/mm	420	Maximum drilling hole width/mm	350
Rotational speed of cutterhead/rpm	200–240	Minimum drilling hole length/mm	450
Maximum drilling hole depth/mm	350	Minimum throwing soil distance/mm	500

## 2.2. Consumption Analysis of Soil Cutting Based on Multi-Body Dynamics

### 2.2.1. Smooth Particle Hydrodynamics (SPH) Algorithm

In soil cutting research, empirical formula calculations or experiments are generally used to analyze the hole-digging resistance and power consumption characteristics. When faced with complex operation modes and external conditions, the results obtained by these methods will have a large error, which seriously affects the evaluation of mechanical performance [17,18]. With the improvement of the constitutive soil model, the finite element method has become an effective tool to analyze the interaction between mechanical soil-contacting parts and soil. In this paper, ANSYS/LS-DYNA software is used to simulate and analyze the soil-cutting process of the hole cutter, and SPH (smooth particle hydrodynamics method) is used to establish a soil model to study the interaction mechanism between tool and soil from a microscopic perspective. Therefore, the law of power consumption change in intermittent soil cutting can be obtained [19–21]. The simulation process for intermittent soil cutting is shown in Figure 3.

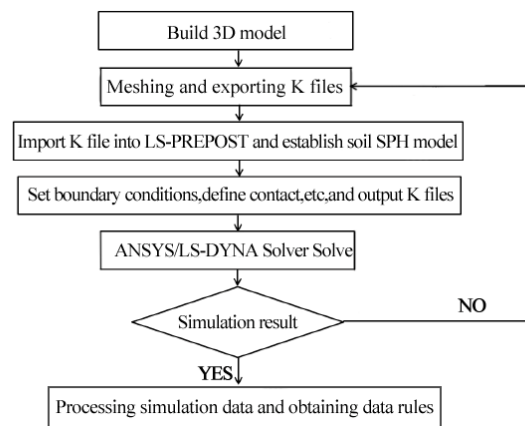


**Figure 3.** Flow chart of soil cutting simulation.

SPH adopts a meshless algorithm, which has great advantages in dealing with the loose fragmentation and separation of the multiphase continuum in the interaction between soil and tool. To correctly characterize the particle motion, this algorithm needs to construct an approximate function representing particle motion information [22–24].

$$\prod^h f(x) = \int f(y)W(x - y, h)dy \quad (1)$$

where ( $W$ ) is the kernel function, and the two independent variables ( $x$ ) and ( $h$ ) are the position vector and the smooth length, respectively. The value of ( $h$ ) directly affects the calculation accuracy, and the kernel function should be a symmetric decreasing function. The attributes of particles will diffuse and affect the surrounding particles, and the influence will gradually decrease with the increase in distance ( $\theta$ ). The kernel function is defined as follows:

$$W(x, h) = \frac{1}{f(x)^v} \theta(x) \quad (2)$$

where ( $v$ ) is the space dimension; ( $h$ ) is the smooth length;  $W(x, h)$  is the spike function.

The most common smooth kernel in SPH is the cubic B-spline, which is defined as follows:

$$\theta(\mu) = \begin{cases} (1 - 1.5\mu^2 + 0.75\mu^3)C & (|\mu| \leq 1) \\ 0.25C(2 - \mu)^3 & (1 < |\mu| < 2) \\ 0 & (2 \leq |\mu|) \end{cases} \quad (3)$$

where ( $C$ ) is a constant (determined by the spatial dimension).

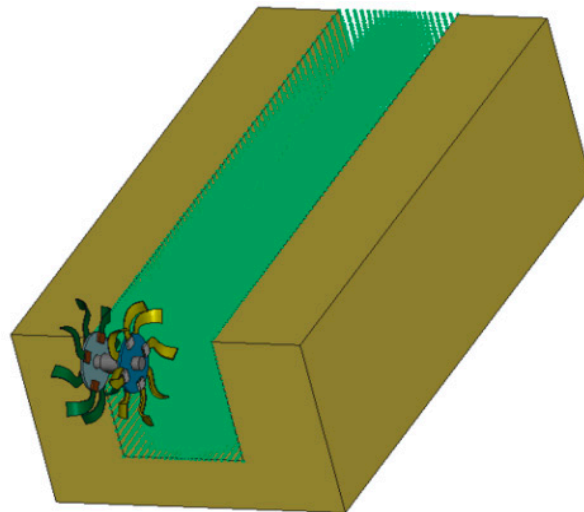
### 2.2.2. Establishment of the Cutterhead—Soil Simulation Model

In this paper, the 3D modeling software Pro/E is used to establish the geometrical model of the hole cutter and soil, and the model size is consistent with the actual size of the hole-digging parts. To improve the computational efficiency without affecting the simulation accuracy, the geometrical model of the transmission system and related devices is reasonably simplified. Specifically, the chamfer, fillet, and other connection features between the blade and the cutter head are omitted. In order to ensure the accuracy of the simulation results, a rigid material was selected for the cutterhead, and the MAT147 (MAT-FHWA\_SOIL) material model provided by ANSYS/LSPREPOST was used as the soil model. The main characteristic parameters of the soil model were measured through actual testing on the test site, including soil density, specific gravity, moisture content, shear modulus, cohesion, bulk modulus, internal friction angle, angle of repose, and Poisson's ratio. The main parameters for the cutterhead and soil are shown in Table 2.

**Table 2.** The parameters of the cutterhead and soil in the test location.

Parameter	Value	Parameter	Value
Elastic modulus/MPa	$1.97 \times 10^5$ (65 Mn)	Rate of water content/%	16
Cutterhead density/(g/cm <sup>3</sup> )	7.85	Soil angle of repose/°	40.5
Poisson's ratio	0.282	Shear modulus/MPa	1.56
Cutterhead diameter/(mm)	420	Cohesion/MPa	0.02
Blade working length/(mm)	125	Bulk modulus/MPa	29
Soil density/(g/cm <sup>3</sup> )	1.73	Internal friction angle/(°)	35.5
Specific gravity	2.62	Soil poisson's ratio	0.4

Considering the intermittent digging action and the boundary condition treatment requirements, a numerical model simulating the interaction of soil and cutter head is established, as shown in Figure 4, and the soil dimensions are 2000 mm, 400 mm, and 500 mm.

**Figure 4.** The simulation model used to analyze the interaction of the cutter head and soil.

### 2.2.3. Boundary Conditions and Loads

According to the actual operating conditions and agronomic requirements, the planting spacing is 3000 mm, the hole-digging depth and width of the target young tree studied are both 350 mm, the tractor speed is 0.25 m/s, the hole-digging cylinder speed is 80 mm/s, and the floating cylinder speed is 19 mm/s. The cutter head speed is set at 200 r/min, 220 r/min, and 240 r/min. The bottom of the soil model is a fixed constraint. The gravity effect is considered in the entire model, and the gravity acceleration is  $-9800 \text{ mm/s}^2$ , which is set according to the solution time. The modified K-file is generated first and transferred to the solver of ANSYS 16.0/LS-DYNA software.

## 3. Results and Discussion

### 3.1. Simulation Results and Analysis

The soil-cutting process of the hole cutter is shown in Figure 5. Once the LS-DYNA solution was completed in LS\_PREPOST, the process of intermittent cutting of the soil by the digging parts was observed, and the data and curves of stress change and energy change between the cutting device and the soil were obtained.

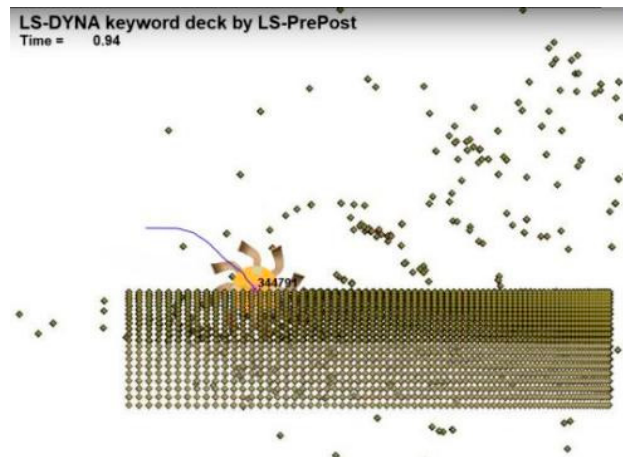


**Figure 5.** Soil-cutting process of digging components.

The power consumption curve of the digging process is shown in Figure 6. The simulation results show that the impact of the rotating speed on power consumption is relatively significant. The higher the rotating speed, the higher the power consumption, which is not obvious at the initial stage of digging. The power consumption value increases rapidly with the depth of the digging part. The main reason is that as the amount of soil being cut increases continuously, the amount of disturbed and returned soil also increases. The high rotating speed of the cutter head and the large kinetic energy obtained by the soil lead to high energy consumption.

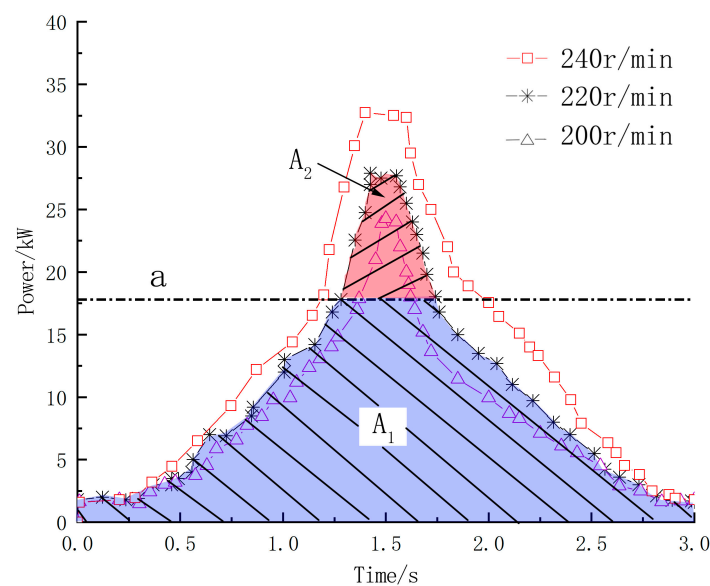


**Figure 6.** Power consumption curve during digging.

Since the cutter head speed of 220 r/min is conducive to the subsequent soil covering operation, this paper focuses on analyzing power consumption change characteristics at this speed. The digging parts contact the soil according to the mechanism's operation track. At the start, because the digging parts only cut a small amount of surface soil, the power has increased slightly. After 0.5 s, the hole-digging knife will penetrate deeper into the soil, and more blades will simultaneously act on the soil. The soil will be broken due to extrusion deformation. A significant amount of energy will be consumed at this time, and the power will increase rapidly. After 1.28 s, the hole digging depth is relatively large. Most of the hole-digging blades simultaneously work on the soil. A large amount of cut soil needs to be thrown to the rear and both sides. Hence, the total power consumption increases rapidly.

The hole digging depth reaches 350 mm at 1.44 s, and the maximum power is 27.93 kW. Then, the digging parts run upward, and the power consumption decreases slowly. After 1.55 s, the power consumption drops sharply, caused by the small amount of soil cut by the tool during the return trip. The soil to be cut is damaged, and the binding force of soil particles decreases, causing the failure to soften.

### 3.2. Flywheel Power Compensation Strategy and Flat Torque Analysis

#### 3.2.1. Power Compensation Scheme Based on Simulation Results

The schematic diagram of intermittent cavity digging is shown in Figure 7. The operation is characterized by long-time low-load operation of the machine; the plant distance ( $L$ ) is generally large and the spike load appears in a short time. A series of faults often occur in the actual operation, such as unreasonable power matching, low efficiency, poor operation effect, no digging, no pulling, high energy consumption, and power output shaft breaking. The torque fluctuation of the transmission system should be minimized during large-area transplant operations. The selected tractor should work close to full load so that power can be effectively used and fuel can be saved.

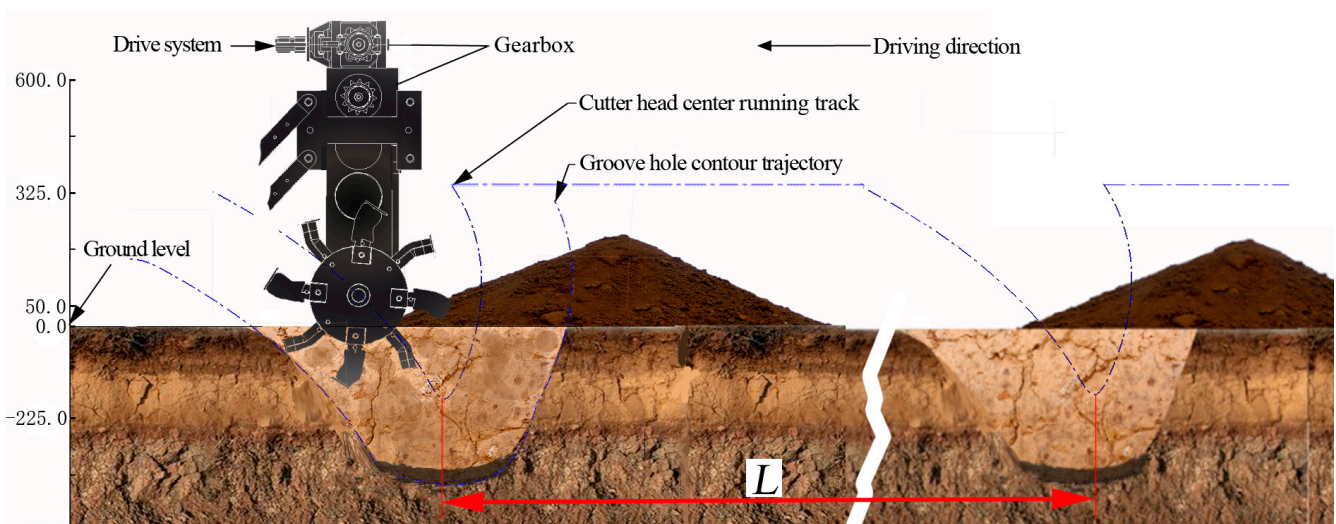


Figure 7. Diagram of intermittent digging.

According to the simulation analysis results, when the rotating speed of the cutter head is 220 r/min, the area enclosed by the power consumption curve and the coordinate axis is the energy required for a planting cycle. The curve is flat before 1.28 s, after which the power increases sharply and reaches 27.93 kW. Then, the power drops sharply. There is a short-time peak with a time of only 0.46 s, and the power suddenly increases by 10.11 kW, which has an obvious short-time peak characteristic. According to the operational characteristics of the mechanical energy storage system, the compensation peak energy of flywheel intervention is satisfied at this stage. The abscissa of the intersection point of the straight line (a) and the curve is the flywheel intervention's start and end time, and the flywheel's total energy to be compensated by the flywheel is  $A_2$ . Therefore, this paper will use the power value (17.82 kW) corresponding to the straight line (a) as the basis for tractor selection, and the energy storage flywheel will compensate for the excess energy. With this scheme, the output power of the power output shaft can be reduced by 36.2% compared with that without the flywheel.

#### 3.2.2. Design of Energy Storage Flywheel and Analysis of Torque Fluctuation

By calculating the area of  $A_2$  shown in Figure 6, the energy compensated by the energy storage flywheel is about 2382.5 J. Considering the effect of soil throwing, the maximum

allowable speed reduction of the cutter head is 10%. The other parameters are the same as the simulation parameters. The moment of inertia is obtained by the following equation:

$$E_{c.fw} = \frac{1}{2}J_{fw}\omega_1^2 - \frac{1}{2}J_{fw}\omega_2^2 \quad (4)$$

where ( $E_{c.fw}$ ) is flywheel compensation energy,  $J$ ; ( $J_{fw}$ ) is flywheel rotational inertia; ( $\omega_1$ ) is the angular velocity at the start of flywheel output energy; and ( $\omega_2$ ) is the angular velocity at the end of flywheel output energy.

The flywheel speed cannot be excessive. The flywheel material is an isotropic metal material. The processing technology is mature, and the price is low. The flywheel is made of metal. Based on the flywheel optimal control theory, the low-speed and hollow flywheel is used for structural design and optimization. The structure scheme of the energy storage flywheel system is shown in Figure 8. The system is composed of a pair of identical flywheels. After calculation, the rotational inertia of a single flywheel is  $1.85/\text{kg}/\text{m}^2$ , in which the flywheel diameters  $D_2$ ,  $D_3$ , and  $D_4$  and the flywheel thickness  $B$  (which are not detailed here) are determined according to the flywheel material and the structural parameters of the transplanter.

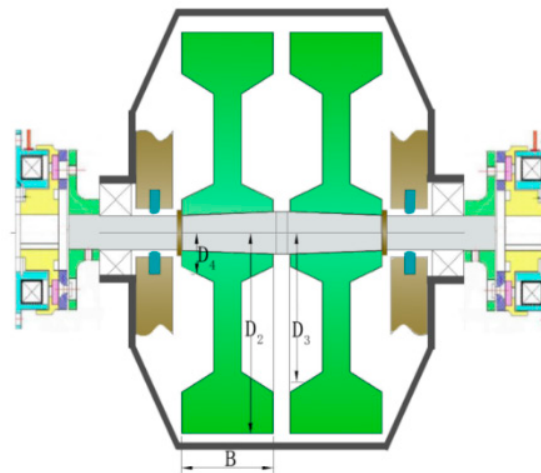


**Figure 8.** Diagram of the energy storage flywheel system.

After the energy storage flywheel of the transmission system is connected in series, in order to study the torque fluctuation of the transmission system, the main parameters of the transmission system are solved based on the simulation results and the flywheel parameters according to the speed ratio of the power output shaft to the cutter head of 36:11, the transmission efficiency of 0.92, and the maximum speed reduction of the flywheel energy release of 10%. Consequently, the PTO output torque and speed change diagram shown in Figure 9 are obtained. In a work cycle, the resistance torque is represented by  $T_{z1}$  and  $T_{z2}$ , respectively, in the two stages of cutting soil and idling, and the PTO output torque is represented by  $T_e$ . The drive system has a flywheel, which plays the role of storing and releasing energy. When digging and cutting the soil, the power output torque of the power output shaft works on the soil at the initial stage. At 1.28 s, due to a sudden increase in resistance, the flywheel speed decreases and starts to release energy for torque compensation. Finally, the flywheel speed decreases to  $\omega_2$ . The resistance torque decreases at 1.74 s, and the flywheel starts to absorb energy. With a decrease in resistance torque, the flywheel absorbs energy rapidly. After 3.55 s, the flywheel speed is  $\omega_1$  (720 r/min), and the energy released by the flywheel is equal to the energy absorbed during the hole-digging process, i.e.,  $A_2 = A_2'$ . It can be seen from the figure that the maximum output torque of the power output shaft without the flywheel system is 445.7 N·m. In contrast, the maximum torque with the flywheel system is 285.1 N·m, i.e., the torque is reduced by 160.6 N·m. The torque fluctuation of the transmission system is greatly reduced. In the figure, ( $n$ ) is the

flywheel speed. When the system torque surges at 1.28 s, the flywheel releases energy and slows down by 10% ( $\omega_2$ ). After that, it absorbs energy and accelerates with the transmission system. This process accelerates faster in the later stages.

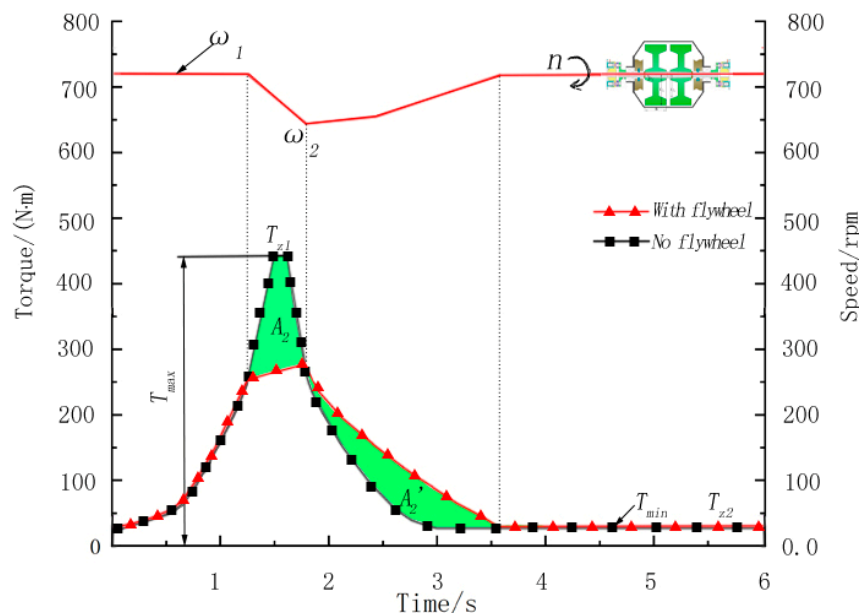


**Figure 9.** PTO output torque variation diagram.

### 3.3. Performance Testing

#### 3.3.1. Test Preparation

A test system for the power consumption of the transplanting machine digging holes is built, and the field digging experiments are carried out to verify the accuracy of the simulation results and further analyze the power change after the series flywheel system, as shown in Figure 10. The main test equipment is the Dongfanghong 504-1 tractor, in which the engine rated power and speed are 35 kW at 2300 r, the maximum torque speed is 1500–1700 r/min, the power output shaft speeds are 720 r/min and 1000 r/min, the transplanter prototype (because of the research on intermittent digging power consumption in this paper, the transplanter will remove the young tree planting and soil covering compaction mechanism), the JN-DN3-1500 N·m rotary (dynamic) torque sensor, and the 24 DV/500 mA power supply Intelligent display controller ( $\pm 0.05\%$  FS) and data processing equipment. The (dynamic) torque sensor is installed between the flywheel and the power take-off, and the intelligent display controller is fixed below it. First, the field test was carried out without the flywheel, focusing on the system power change after the flywheel was installed. The test was conducted on 5 October 2022 at the experimental field of Northeast Forestry University in Heilongjiang Province, located in the central part of the Songnen Plain. The geographical coordinates are  $126^{\circ}5'$  E and  $45^{\circ}5'$  N, and the experimental terrain is sloping with a maximum slope angle of less than  $8^{\circ}$ . It needs to be emphasized that the tree planter can adapt to most terrain. If it encounters obstacles such as thick tree roots or large stones, the controller will cut off the electromagnetic clutch after detecting the signal, and the planting mechanism will rise above the ground. The saplings used in the experiment were Lesser Black Poplar, with an average height of about 2 m and an average ground diameter of about 1.5 cm. The soil characteristic parameters of the test site are shown in Table 2. The slip rate of rubber tires is 5%–8% when plowing on the test site. The driving speed in the test study is the actual driving speed of the transplanter after considering the tire slip rate.



**Figure 10.** Field experiment. (a) Intermittent hole digging and tree planting machine (b) Test system and planting.

During the test, the digging depth is 350 mm, the power output shaft and cutter head speed ratio is 36:11, and the cutter head speed is set at 200 r/min, 220 r/min, and 240 r/min, respectively. The movement parameters of the transplanter are the same as the simulation parameters. The clutch is smoothly combined during the test to rotate the transmission system at a low speed. Then, slowly control the throttle until the MCK-Z intelligent display control instrument displays the power output shaft speed in real-time. The sensor obtains the torque data during the digging process in real-time. The change in torque output by the transmission shaft directly reflects the power consumption of the digging system. See Formula (5) for the power change.

$$P = \frac{T_e n}{9549} \quad (5)$$

where ( $P$ ) is the power consumption of digging process, kW; ( $n$ ) is the speed of digging cutter, r/min.

### 3.3.2. Test Results and Analysis

Considering the influence of unknown factors on the system test results, each group of tests was carried out randomly. A total of 10 groups of tests were carried out. Each group of tests completed six pits in succession. The test data corresponding to two consecutive tree-planting pits in the middle were selected, and the measured results were taken as the average. In the test without a flywheel, the maximum value displayed by the torque sensor was 454.6 N·m, which is similar to the simulation and theoretical solution. Figure 11 shows the power consumption curve of the test digging process. The measured power values at three speeds are higher than the simulation results. The main reason is that the speed of the flywheel is reduced during power compensation. As the load increases, the power of the power output shaft increases, i.e., the energy released by the flywheel and the engine act together at the peak load, and the energy released by the flywheel accounts for a large proportion. When the cutter head speed is 200 r/min, the power output shaft's power fluctuation is small. The rotating speed of the cutter head is 240 r/min, the power fluctuates, and the driving speed of the tractor is unstable. The main reason is that the rotating speed is high and the work done by throwing soil has increased. Even though the flywheel energy storage increases, it is still lower than the energy consumption increased by digging and throwing soil. The enclosed areas of the power consumption curve and a line at different speeds are  $S_1$ ,  $S_2$ , and  $S_3$ . The higher the speed, the higher the actual output energy of the engine power output shaft. The three points,  $A$ ,  $B$ , and  $C$ , are the maximum power consumption coordinate points corresponding to the cutter head speed at 240 r/min, 220 r/min, and 200 r/min, respectively, during the simulation analysis without a flywheel. The field test results show that the output power of the power output shaft decreases significantly once the flywheel system is added, i.e., by 10.54 kW, 10.11 kW, and 5.82 kW with respect to different cutter head speeds. The test results also show that the maximum output power peak will move backward when the flywheel is installed in

the transmission system. The output power will decline slowly and then rapidly, mainly because the flywheel needs to store energy when accelerating with the transmission system. When the cutter head cuts the soil at 220 r/min, the lowest flywheel speed measured is 656 r/min. The speed decreases by 8.9%, which is 1.1% lower than the simulated value.

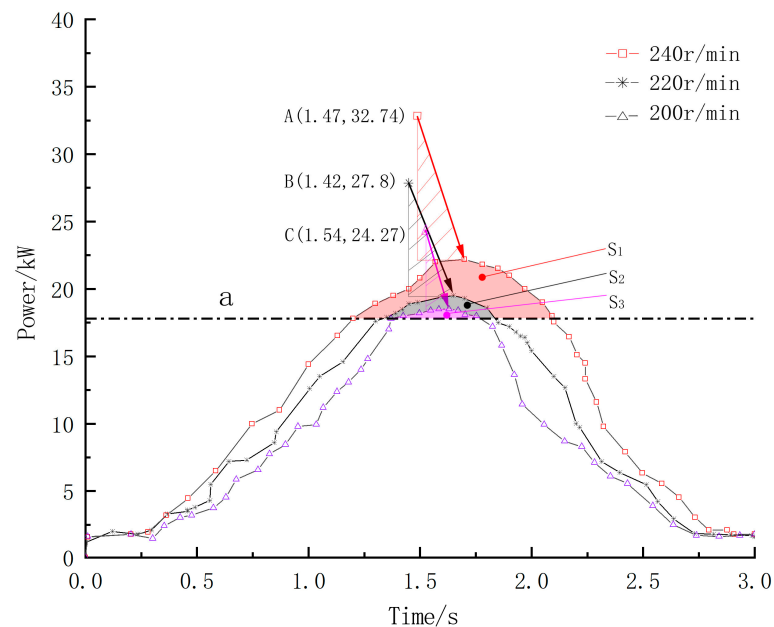


**Figure 11.** Power consumption curve during experimental digging.

#### 4. Conclusions

This paper mainly studies the power compensation strategy of the tree-planting machine transmission system after installing an energy storage flywheel. The expected results have been achieved through theoretical, simulation, and experimental research. Achieved smoother output power from the driving unit. Tree planting machines allow for the use of more power-matched and lower drive units, reducing energy consumption and exhaust emissions. A non-linear multi-body dynamics simulation model of soil cutting by digging parts is first established, and boundary conditions and contact conditions are set to simulate the power consumption of the digging process. The simulation results show that the higher the speed, the higher the power consumption. When the speed is 220 r/min, the power increases from 17.82 kW (1.28 s) to 27.93 kW (1.43 s), and then decreases rapidly after the peak, and the power consumption shows short-time spikes. According to the simulation results of power consumption curve characteristics, the total compensation energy is 2382.5 J. Because of the flywheel system, the torque fluctuation of the tree planting machine reduces by 160.6 N·m. Field test results are similar to the simulation results; the test shows that the energy required to overcome the spike load is provided by the flywheel and engine together; when the digging parts speed is 220 r/min, the actual power input to the power output shaft during the energy release of the flywheel system was 18.51 kW, with an error of 2.43% compared to the simulated value, i.e., the input power was reduced by 9.42 kW after the flywheel was installed, and the actual speed reduction of the flywheel system was measured to be 8.9%. There are still issues with studying the installation of energy storage flywheels in tree planting machines to achieve energy collection and compensation. In our future work, we will continue to study the electromagnetic coupling flywheel energy storage system and topology optimization of flywheel structure, focusing on researching and improving the energy utilization rate of afforestation equipment.

**Author Contributions:** Conceptualization and methodology, J.L. and C.Y.; writing—original draft preparation, B.Z., W.Q. and P.D.; formal analysis, J.L. and B.Z.; writing—review and editing, B.Z., P.D. and J.L. All authors have read and agreed to the published version of the manuscript.

**Funding:** This research was funded by The National Key Research and Development Program of China (No.2022YFD2202101).

**Data Availability Statement:** Not applicable.

**Conflicts of Interest:** The authors declare no conflict of interest.

## References

1. Turchetto, F.; Araujo, M.M.; Tabaldi, L.A.; Griebeler, A.M.; Rorato, D.G.; Aimi, S.C.; Berghetti, L.; Gomes, D.R. Can transplantation of forest seedlings be a strategy to enrich seedling production in plant nurseries? *For. Ecol. Manag.* **2016**, *375*, 96–104. [[CrossRef](#)]
2. Chen, D.; Hou, J.; Shi, G. Analysis on the current situation of technology of domestic dryland transplanter. *J. Chin. Agric. Mech.* **2018**, *39*, 98–102. [[CrossRef](#)]
3. Warguła, L.; Lijewski, P.; Kukla, M. Effects of Changing Drive Control Method of Idling Wood Size Reduction Machines on Fuel Consumption and Exhaust Emissions. *Croat. J. For. Eng.* **2023**, *44*, 137–151. [[CrossRef](#)]
4. Laitila, J.; Routa, J. Performance of a small and a medium sized professional chippers and the impact of storage time on Scots pine (*Pinus sylvestris*) stem wood chips characteristics. *Silva Fenn.* **2015**, *49*, 1382. [[CrossRef](#)]
5. Lu, J. Analysis on the development trend of energy conservation and emission reduction of oil drilling diesel engines. *China Pet. Chem. Stand. Qual.* **2021**, *41*, 118–119. [[CrossRef](#)]
6. Patel, T.; Chakravorty, A.; Karmakar, S. Software for performance prediction and matching of tractor-implement system. In Proceedings of the 2012 3rd National Conference on Emerging Trends and Applications in Computer Science, Shillong, India, 30–31 March 2012; pp. 262–269. [[CrossRef](#)]
7. Song, D.; Wang, Z.; Zhang, Y. Overview of the development of ecological transplanters. *For. Mach. Wood-Work. Equip.* **2004**, *32*, 4–6. [[CrossRef](#)]
8. Savickas, D.; Steponavičius, D.; Domeika, R. Analysis of Telematics Data of Combine Harvesters and Evaluation of Potential to Reduce Environmental Pollution. *Atmosphere* **2021**, *12*, 674. [[CrossRef](#)]
9. Savickas, D.; Steponavičius, D.; Špokas, L.; Saldukaitė, L.; Semenišin, M. Impact of Combine Harvester Technological Operations on Global Warming Potential. *Appl. Sci.* **2021**, *11*, 8662. [[CrossRef](#)]
10. Janulevičius, A.; Juostas, A.; Pupinis, G. Tractor's engine performance and emission characteristics in the process of ploughing. *Energy Convers. Manag.* **2013**, *75*, 498–508. [[CrossRef](#)]
11. Itani, K.; De Bernardinis, A.; Khatir, Z.; Jammal, A. Comparative analysis of two hybrid energy storage systems used in a two front wheel driven electric vehicle during extreme start-up and regenerative braking operations. *Energy Convers. Manag.* **2017**, *144*, 69–87. [[CrossRef](#)]
12. Guney, M.S.; Tepe, Y. Classification and assessment of energy storage systems. *Renew. Sustain. Energy Rev.* **2017**, *75*, 1187–1197. [[CrossRef](#)]
13. Liu, F.; Li, J.; Li, Y. Research and application demonstration of magnetic levitation energy storage flywheel technology. *Shanghai Energy Conserv.* **2017**, *338*, 80–84. [[CrossRef](#)]
14. Dai, X.; Wei, K.P.; Zhang, X. Fifty year review of flywheel energy storage technology research. *Energy Storage Sci. Technol.* **2018**, *7*, 765–782. [[CrossRef](#)]
15. Hannan, M.A.; Azidin, F.; Mohamed, A. Hybrid electric vehicles and their challenges: A review. *Renew. Sustain. Energy Rev.* **2014**, *29*, 135–150. [[CrossRef](#)]
16. Wang, H.; Wei, Q.; Du, J. Development trend of energy conservation and emission reduction of oil drilling diesel engines. *Plant Maint. Eng.* **2017**, *407*, 142–144. [[CrossRef](#)]
17. Kang, J.; Li, S.; Yang, X. Virtual simulation and power test of disc type ditcher based on multi-body dynamics. *Trans. Chin. Soc. Agric. Mach.* **2017**, *48*, 57–63. [[CrossRef](#)]
18. Chen, L.; Liang, X.; Cao, C. Virtual simulation and power test of straw counters-field based on multi-body dynamics. *Trans. Chin. Soc. Agric. Mach.* **2016**, *47*, 106–111. [[CrossRef](#)]
19. Guo, X.; Tang, L.; Zeng, X. Numerical simulation of soil cutting based on ansys/lS-dyna rotary tillage tool. *Sichuan Agric. Mach.* **2016**, *209*, 42–43. [[CrossRef](#)]
20. Cao, Z.; Cui, J.; Zhan, X. Simulation and experimental study of soil cutting process by subsoiler based on SPH method. *J. Agric. Mech. Res.* **2019**, *41*, 28–34+41. [[CrossRef](#)]
21. Lu, C.; He, J.; Li, H. Simulation of soil cutting process by plane blade based on SPH method. *Trans. Chin. Soc. Agric. Mach.* **2014**, *45*, 134–139. [[CrossRef](#)]
22. Cavoretto, R.; De Rossi, A. A meshless interpolation algorithm using a cell-based searching procedure. *Comput. Math. Appl.* **2014**, *67*, 1024–1038. [[CrossRef](#)]

23. Korzani, M.G.; Galindo-Torres, S.; Scheuermann, A.; Williams, D. Smoothed Particle Hydrodynamics for investigating hydraulic and mechanical behaviour of an embankment under action of flooding and overburden loads. *Comput. Geotech.* **2017**, *94*, 31–45. [[CrossRef](#)]
24. Stevens, D.; Power, H.; Morvan, H. An order-N complexity meshless algorithm for transport-type PDEs, based on local Hermitian interpolation. *Eng. Anal. Bound. Elem.* **2009**, *33*, 425–441. [[CrossRef](#)]

**Disclaimer/Publisher’s Note:** The statements, opinions and data contained in all publications are solely those of the individual author(s) and contributor(s) and not of MDPI and/or the editor(s). MDPI and/or the editor(s) disclaim responsibility for any injury to people or property resulting from any ideas, methods, instructions or products referred to in the content.